HHS Public Access

Author manuscript

Biochem Biophys Res Commun. Author manuscript; available in PMC 2022 May 21.

Published in final edited form as:

Biochem Biophys Res Commun. 2021 May 21; 554: 145–150. doi:10.1016/j.bbrc.2021.03.091.

Tau induces formation of α-synuclein filaments with distinct molecular conformations

Alimohammad Hojjatian[1], **Anvesh K. R. Dasari**[2], **Urmi Sengupta**[3], **Dianne Taylor**[1], **Nadia Daneshparvar**[1], **Fatemeh Abbasi Yeganeh**[1], **Lucas Dillard**[4], **Brian Michael**[5], **Robert G. Griffin**[5], **Mario Borgnia**[4], **Rakez Kayed**[3], **Kenneth A. Taylor**[1], **Kwang Hun Lim**[2]

[1]Institute of Molecular Biophysics, Florida State University, Tallahassee, FL 32306-4380, USA

[2]Department of Chemistry, East Carolina University, Greenville, NC 27858, USA

[3]Departments of Neurology, Neuroscience and Cell Biology, University of Texas Medical Branch, Galveston, TX, 77555, USA

[4]Genome Integrity and Structural Biology Laboratory, National Institute of Environmental Health Sciences, National Institutes of Health, Research Triangle Park, NC, 27709, USA

[5]Department of Chemistry and Francis Bitter Magnet Laboratory, Massachusetts Institute of Technology, Cambridge, MA, 02139, USA

Abstract

Recent structural investigation of amyloid filaments extracted from human patients demonstrated that the ex vivo filaments associated with different disease phenotypes adopt diverse molecular conformations, which are different from those of in vitro amyloid filaments. A very recent cryo-EM structural study also revealed that ex vivo α-synuclein filaments extracted from multiple system atrophy patients adopt distinct molecular structures from those of in vitro α-synuclein filaments, suggesting the presence of co-factors for α-synuclein aggregation in vivo. Here, we report structural characterizations of α-synuclein filaments formed in the presence of a potential co-factor, tau, using cryo-EM and solid-state NMR. Our cryo-EM structure of the tau-promoted α-synuclein filaments reveals some similarities to one of the previously reported polymorphs of in vitro α-synuclein filaments in the core region, while illustrating distinct conformations in the N- and C-terminal regions. The structural study highlights the conformational plasticity of α-synuclein filaments and the importance of the co-factors, requiring additional structural investigation of not only more ex vivo α-synuclein filaments, but also in vitro α-synuclein filaments formed in the presence of diverse co-factors. The comparative structural analyses will help better understand molecular basis of diverse structures of α-synuclein filaments and possible relevance of each structure to the disease phenotype.

Graphical Abstract

Corresponding authors: limk@ecu.edu.

Conflicts of interest

The authors have no conflicts of interest to declare.

Appendix A. Supplementary Data

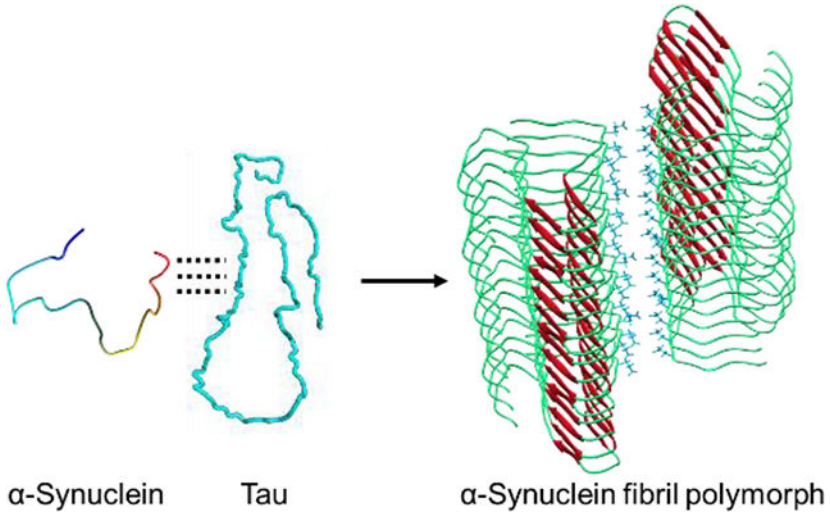

Keywords

α-Synuclein; cryo-EM; tau; solid-state NMR

1. Introduction

Aggregation of α-synuclein into amyloid filaments is associated with numerous neurodegenerative diseases including Parkinson's disease (PD), dementia with Lewy bodies (DLB), and multiple system atrophy (MSA) collectively termed synucleinopathy [1]. Increasing evidence suggests that the protein aggregates play a key role in the initiation and spreading of pathology in the neurodegenerative diseases [2, 3]. It was shown that α-synuclein aggregates are capable of spreading through the brain and acting as seeds to promote misfolding and aggregation like prion [4, 5]. In addition, injection of preformed filamentous α-synuclein aggregates into mice induced PD-like pathology [4, 6]. Structural elucidation of filamentous α-synuclein aggregates is, therefore, essential to understanding molecular basis of neurotoxic properties of α-synuclein aggregates and developing therapeutic strategies.

α-synuclein is a 140-residue protein expressed predominantly in the dopaminergic neurons [7]. The intrinsically disordered protein adopts heterogeneous ensembles of conformations. The diverse conformers in the conformational ensemble might be induced to form distinct amyloid aggregates with different molecular conformations depending on experimental conditions [5, 8]. Indeed, recent high-resolution structural studies using solid-state NMR and cryo-EM revealed that α-synuclein filaments can adopt diverse molecular conformations under various in vitro experimental conditions [9–14]. Structural analyses of α-synuclein aggregates seeded by brain extracts from PD and MSA patients also suggested that the brain-derived aggregates are heterogenous mixtures of filaments that are distinct from in vitro α-synuclein filaments [15]. Very recently, high-resolution cryo-EM structures of α-synuclein filaments extracted from MSA and DLB patients were reported [16]. Interestingly, two types of α-synuclein filaments consisting of two asymmetric protofilaments were

observed in MSA filaments extracted from 5 patients. On the other hand, ex vivo DLB filaments were untwisted and morphologically different from those of ex vivo MSA. The structural studies revealed that ex vivo α-synuclein filaments are structurally diverse and quite distinct from those of in vitro α-synuclein filaments produced in buffer, suggesting that diverse co-factors may exist in vivo and induce formation of different α-synuclein filaments.

α-synuclein remains largely unfolded at low protein concentrations (< 0.1 mM) under physiological conditions. The formation of filamentous aggregates is triggered at aggregation-prone conditions such as higher protein concentrations and more acidic pH [8]. Misfolding and aggregation of α-synuclein is also promoted by interactions with a variety of co-factors such as lipids, poly(ADP-ribose) (PAR), and other pathological aggregation-prone proteins such as tau and Aβ(1–42) peptides [8, 17–20]. The co-factors may interact with monomeric α-synuclein and lead to distinct misfolding pathways, resulting in different molecular conformations. Comparative structural analyses of in vitro α-synuclein filaments formed in the presence of co-factors and brain-derived ex vivo α-synuclein filaments are required to identify co-factors that promote α-synuclein aggregation in vivo.

Our previous NMR study revealed that tau interacts with the C-terminal region of α-synuclein, accelerating the formation of α-synuclein filaments [21]. Here we report structural investigation of the tau-promoted α-synuclein filaments using solid-state NMR and cryo-EM to investigate the effect of the interactions on the structure of α-synuclein filaments. Our initial solid-state NMR studies indicate that the tau-promoted α-synuclein filaments have similar structural features to those of one of the polymorphs. However, cryo-EM structure of the tau-promoted α-synuclein filaments at 4.0 Å resolution revealed distinct molecular conformations in the N- and C-terminal regions with a much faster helical twist, suggesting that the co-factor, tau, directs α-synuclein into a distinct misfolding and aggregation pathway.

2. Materials and Methods

2.1. Protein expression and purification

α-Synuclein: Full-length α-synuclein was expressed in BL21(DE3) *E. coli* cells using pET21a plasmid (a gift from Michael J Fox Foundation, Addgene plasmid # 51486) and was purified at 4 °C as previously described [22]. Briefly, the transformed *E. coli* cells were grown at 37 °C in LB medium to an OD_{600} of 0.8. The protein expression was induced by addition of IPTG to a final concentration of 1 mM and the cells were harvested by centrifugation after 12 hrs of incubation at 25 °C. The bacterial pellet was resuspended in lysis buffer (20 mM Tris, 150 mM NaCl, pH 8.0) and sonicated at 4 °C. The soluble fraction of the lysate was precipitated with ammonium sulfate (50%). The resulting protein pellet collected by centrifugation at 5000 g was resuspended in 10 mM tris buffer (pH 8.0) and the protein solution was dialyzed against 10 mM tris buffer overnight at 4 °C. α-Synuclein was purified by anion exchange chromatography (HiTrap Q HP; 20 mM tris buffer, pH 8) and size exclusion chromatography (HiLoad 16/60 Superdex 75 pg) at 4 °C.

Tau: Recombinant full-length tau (2N4R) protein was expressed and purified from BL21(DE3) *E. coli* cells transformed with the pET15b plasmid (a gift from Dr. Smet-Nocca,

Université de Lille, Sciences et Technologies, France) as previously described [23]. Briefly, when the cells were grown at 37 °C in LB medium to an OD of 0.8, they were induced by addition of 0.5 mM IPTG and incubated for 3–4 hrs at 37 °C. After the induction, the cells were harvested by centrifugation. The bacterial pellet was resuspended in the lysis buffer and sonicated at 4 °C. The soluble fraction was heated at 80 °C for 20 min and the precipitates were removed by centrifugation. The supernatant containing tau protein was purified by cation exchange chromatography (HiTrap SP HP; 20 mM MES, 2 mM DTT, 1 mM $MgCl_2$, 1 mM EGTA, 1 mM PMSF) followed by size exclusion chromatography (HiLoad 26/60 Superdex 200 pg).

2.2. Preparation of tau promoted α-synuclein filaments

To prepare α-synuclein filaments in the presence of tau, monomeric α-synuclein (70 μM in 10 mM phosphate buffer, pH 7.4) was mixed with tau monomers (20 μM in 10 mM phosphate buffer, pH 7.4) and incubated at 37 °C for 1 day under constant agitation at 250 rpm in an orbital shaker. Filamentous aggregates were examined with transmission electron microscopy (TEM).

2.3. TEM

A five microliter of α-synuclein filamentous solution (0.01 mg/ml) was placed on a formvar/carbon supported 400 mesh copper grid. After 30 sec incubation of the sample on the TEM grid, excess sample was blotted off with a filter paper. The samples were stained with 10 μL of 1% uranyl acetate for 30 sec and the excess stain was blotted off with a filter paper. The grids were then allowed to air dry and TEM images were collected using a Philips CM12 transmission electron microscope at an accelerating voltage of 80 kV.

2.4. Solid-state NMR

Doubly $^{13}C/^{15}N$-labeled tau-promoted α-synuclein filaments were directly packed into a 3.2 mm magic angle spinning (MAS) rotor by ultracentrifugation at 175,000 × *g* for 4 hours. Two-dimensional solid-state NMR experiments were performed on a Bruker 800 MHz (18.8 T) spectrometer with a 3.2 mm MAS probe.

2.5. Cryo-EM data collection

A four microliter α-synuclein filamentous solution was applied to the back of each of the glow-discharged R2/1 Quantifoil grids. The grids were manually plunge-frozen into liquid nitrogen temperature cooled liquid ethane, after 3 seconds of blotting with filter papers. Grids were examined on Titan Krios electron microscope, equipped with GATAN K3 camera operated at 300kV. The defocus on camera was set to be randomly within 5,000–25,000Å range. The images have been collected with GATAN automated data collection software Latitude S (GATAN, Inc). The magnification was set to 81,000 and as a result the nominal pixel size is set to 1.1Å (the calibrated pixel size is found to be 1.07Å).

3. Results

3.1. Solid-state NMR of the tau-promoted α-synuclein filaments

Monomeric α-synuclein (70 μM) was incubated in the presence of tau monomers (20 μM) at 37 °C in 10 mM phosphate buffer (pH 7.4). Long homogeneous filamentous aggregates were observed after 24 hrs of incubation in the presence of tau (Figure S1). Solid-state NMR was initially used to compare structural features of the tau-promoted filaments to those of previously reported in vitro α-synuclein filaments (Figure 1). The two-dimensional ^{13}C-^{13}C correlation spectrum obtained with a dipolar-assisted rotational resonance mixing scheme (DARR) [24] suggests that the tau-promoted filaments (Figure 1a) have distinct molecular conformations from those of two α-synuclein filaments (Figure 1c and 1d). On the contrary, the 2D DARR spectrum of the tau-promoted filaments is somewhat similar to that of the in vitro filament (red in Figure 1b), particularly in the core region (residues 36 – 79) of the previously reported filaments [25]. Notable differences were also observed in the 2D DARR spectra (black in Figure 1b), suggesting that the co-factor, tau, appears to induce the formation of a distinct fibrillar conformation.

3.2. Cryo-EM structure of the tau-promoted α-synuclein filaments

Cryo-EM was then used to determine near-atomic structure of the tau-promoted α-synuclein filaments. Preformed tau-promoted filaments were frozen on a carbon-coated grid and images were acquired at 81,000x magnification on a Titan Krios (300 kV) equipped with a K3 GATAN direct electron detector camera. About 240,000 segments extracted from 1,800 micrographs were analyzed using Relion reference-free two-dimensional (2D) classification. The initial classification analyses revealed one major species in the 2D classes (Figure 2a). The 2D classes show that the protofilaments are twisted around with a crossover distance of 610 Å (Figure 2b) and a helical rise of ~4.8 Å based on the power spectrum (Figure 2c). The left-twisting handedness was determined by cryo-electron tomography. The 2D classes were used for three dimensional (3D) helical reconstruction in Relion 3, which resulted in a 3D density map at 4.0 Å resolution (Figure 3a) (the image processing procedure is described in Supplementary Data).

Our initial solid-state NMR studies indicated that the tau-promoted filaments share structural features with one of the previous α-synuclein filaments (Figure 1a and 1b). Thus, the 3D density map of the tau-promoted α-synuclein filaments was compared to those of the previous α-synuclein filaments (Figure 3). The two α-synuclein filaments have similar molecular conformations (Figure 3d). It is, however, interesting to note that tau induced the formation of only one polymorph (Figure 3a and 3c), although the previous study showed that the protofilaments were assembled into the two fibril polymorphs in the same buffer (Figure 3b and 3c) [13]. The tau-promoted α-synuclein filament also exhibits notable differences in comparison to that of the polymorph, particularly the N- and C-terminal regions (Figure 3d and Figure S2). Firstly, the interaction between the N-terminal (15–20) and C-terminal (85–91) regions could not resolved in the tau-promoted filament reconstruction. Secondly, the more extensive C-terminal region (80–140) is disordered in comparisons with that of the other structure (91–140), which might be due to interactions between the positively charged tau and negatively charged C-terminal region of α-synuclein

(Figure S2). Thirdly, the tau-promoted filaments with a half-pitch of 63 nm are twisted much faster in comparison with that of the polymorph (96 nm) (Figure 3d and Figure S3).

The structural model for the tau-promoted filaments was compared to the other previously reported structures of α-synuclein filaments (Figure 4). Our tau-promoted α-synuclein filaments adopt an overall Greek-key type structure observed in the first solid-state NMR structure of α-synuclein filaments [9]. However, several regions including the N- and C-terminal regions (residues 36–48 and 66–79) are notably different from the previous Greek-key type structures, as was suggested by our solid-state NMR results (Figure 1a and 1d). In addition, interfacial contacts between the two protofilaments and the degree of helical twist (Table S1) are quite distinct from those of the previously reported structures. These results indicate that interactions between co-factors and α-synuclein may lead to distinct molecular conformations and intermolecular contacts between the protofilaments.

4. Discussion

Molecular mechanism by which α-synuclein self-assembles into fibrillar aggregates in vivo has remained largely unknown. It was previously shown that monomeric α-synuclein is stabilized by long-range interactions between the N- and C-terminal regions [26, 27]. Perturbations of the long-range interactions may initiate misfolding and aggregation of α-synuclein. Indeed, various co-factors that interact with the N- and/or C-terminal regions promoted the formation of fibrillar aggregates of α-synuclein [28–30]. Recently solved cryo-EM structures of ex vivo α-synuclein filaments extracted from MSA and DLB patients revealed that the ex vivo filaments adopt distinct molecular structures from those of in vitro α-synuclein filaments [16], supporting that co-factors may play important roles in promoting α-synuclein aggregation in vivo. Comparative structural analyses of α-synuclein aggregates derived by co-factors and ex vivo aggregates will, therefore, be required to identify co-factors that may play critical roles in α-synuclein aggregation in vivo.

Several lines of evidence indicate that pathological proteins such as β-amyloid (Aβ) peptides, tau and α-synuclein synergistically promote their mutual aggregation [17, 31–35]. In particular, co-existence of tau and α-synuclein aggregates in synucleinopathy patient's brains suggests that tau may interact with α-synuclein, accelerating the formation of fibrillar α-synuclein aggregates in vivo. In this work, we solved cryo-EM structure of α-synuclein filaments formed in the presence of tau and compared the structure to those of previously reported structures of α-synuclein filaments. Previous structural studies of α-synuclein filaments revealed that α-synuclein can form diverse filamentous aggregates with distinct molecular conformations (Figure 4). Polymorphic structures were also observed for the filaments formed even in the same buffer [9, 11, 13]. It is plausible that multiple conformers in the conformational ensemble of disordered α-synuclein are able to form diverse α-synuclein filaments with different molecular conformations and/or different interfaces between the protofilaments. Interestingly, the tau-promoted α-synuclein filaments adopt a Greek-key type structure similar to one of the previously reported polymorphic α-synuclein filaments. However, the detailed molecular conformation and the degree of the helical twist are different from those of the polymorphs (Table S1). In addition, recent studies revealed that poly(ADP-ribose) may interact with α-synuclein in vivo [36] and induce the formation

of a more toxic α-synuclein strain with distinct molecular conformations [18]. These results suggest that the interaction between co-factors and α-synuclein may direct the protein to a specific misfolding and aggregation pathway toward the distinct α-synuclein filament, highlighting the importance of cellular environments in protein misfolding and aggregation [5].

Previous structural studies of the full-length and truncated α-synuclein filaments revealed that the C-terminally truncated α-synuclein filaments have an increased helical twist even though the full-length and truncated filaments adopt almost identical core structures [12, 37], suggesting that the negatively charged C-terminal region affects the helical twist in the parallel alignment. Thus, the increased helical twist of the tau-promoted full-length α-synuclein filaments may result from the electrostatic interaction between the positively charged tau and negatively charged C-terminal region of α-synuclein, which may reduce repulsive interactions between the C-terminal regions in the parallel alignment and facilitate the tighter helical twist. The longer disordered C-terminal region (residues 81 – 140) in the tau-promoted filament compared to that of the previously reported α-synuclein filaments (residues 90 – 140) may also result from the interaction between the tau and C-terminal regions of α-synuclein.

In summary, we report a distinct molecular structure of the α-synuclein filament formed in the presence of tau. The interaction between α-synuclein and tau leads to a distinct molecular conformation of α-synuclein filament with a shorter helical pitch. These results suggest that interactions between α-synuclein and various potential co-factors in cellular environments may promote the formation of diverse α-synuclein filaments with different molecular conformations. More extensive comparative structural analyses of in vitro α-synuclein filaments derived by co-factors and ex vivo α-synuclein filaments extracted from the patients are required to better understand molecular mechanism of α-synuclein aggregation in vivo.

Supplementary Material

Refer to Web version on PubMed Central for supplementary material.

Acknowledgment

This work was supported in part by NIH R01 NS097490 (K.H.L.), R01 AG054025 (R.K.) and R01 NS094557 (R.K.). We thank Dr. Jun-yong Choe (East Carolina University) for helpful discussion. We also thank Hamidreza Rahmani for helpful suggestions on molecular dynamics analysis on the atomic model.

Abbreviations

NMR	nuclear magnetic resonance
TEM	transmission electron microscopy
DARR	dipolar assisted rotational resonance
cryo-EM	cryo-electron microscopy

MSA	multiple system atrophy
DLB	dementia with Lewy bodies

References

[1]. Goedert M. Alpha-synuclein and neurodegenerative diseases, Nat. Rev. Neurosci 2 (2001) 492–501. [PubMed: 11433374]

[2]. Jucker M, Walker LC. Self-propagation of pathogenic protein aggregates in neurodegenerative diseases, Nature 501 (2013) 45–51. [PubMed: 24005412]

[3]. Frost B, Diamond MI. Prion-like mechanisms in neurodegenerative diseases, Nat Rev Neurosci 11 (2010) 155–9. [PubMed: 20029438]

[4]. Luk KC, Kehm V, Carroll J, Zhang B, O'Brien P, Trojanowski JQ, Lee VM. Pathological alpha-synuclein transmission initiates parkinson-like neurodegeneration in nontransgenic mice, Science 338 (2012) 949–953. [PubMed: 23161999]

[5]. Peng C, Gathagan RJ, Covell DJ, Medellin C, Stieber A, Robinson JL, Zhang B, Pitkin RM, Olufemi MF, Luk KC, Trojanowski JQ, Lee VM. Cellular milieu imparts distinct pathological alpha-synuclein strains in alpha-synucleinopathies, Nature 557 (2018) 558–563. [PubMed: 29743672]

[6]. Sacino AN, Brooks M, Thomas MA, McKinney AB, Lee S, Regenhardt RW, McGarvey NH, Ayers JI, Notterpek L, Borchelt DR, Golde TE, Giasson BI. Intramuscular injection of alpha-synuclein induces CNS alpha-synuclein pathology and a rapid-onset motor phenotype in transgenic mice, Proc. Natl. Acad. Sci. U. S. A 111 (2014) 10732–10737. [PubMed: 25002524]

[7]. Spillantini MG, Schmidt ML, Lee VM, Trojanowski JQ, Jakes R, Goedert M. Alpha-synuclein in lewy bodies, Nature 388 (1997) 839–840. [PubMed: 9278044]

[8]. Stephens AD, Zacharopoulou M, Kaminski Schierle GS. The cellular environment affects monomeric α-synuclein structure, Trends Biochem. Sci 44 (2019) 453–466. [PubMed: 30527975]

[9]. Tuttle MD, Comellas G, Nieuwkoop AJ, Covell DJ, Berthold DA, Kloepper KD, Courtney JM, Kim JK, Barclay AM, Kendall A, Wan W, Stubbs G, Schwieters CD, Lee VM, George JM, Rienstra CM. Solid-state NMR structure of a pathogenic fibril of full-length human alpha-synuclein, Nat. Struct. Mol. Biol 23 (2016) 409–415. [PubMed: 27018801]

[10]. Li Y, Zhao C, Luo F, Liu Z, Gui X, Luo Z, Zhang X, Li D, Liu C, Li X. Amyloid fibril structure of alpha-synuclein determined by cryo-electron microscopy, Cell Res. 28 (2018) 897–903. [PubMed: 30065316]

[11]. Li B, Ge P, Murray KA, Sheth P, Zhang M, Nair G, Sawaya MR, Shin WS, Boyer DR, Ye S, Eisenberg DS, Zhou ZH, Jiang L. Cryo-EM of full-length alpha-synuclein reveals fibril polymorphs with a common structural kernel, Nat. Commun 9 (2018) 3609–2. [PubMed: 30190461]

[12]. Ni X, McGlinchey RP, Jiang J, Lee JC. Structural insights into alpha-synuclein fibril polymorphism: Effects of parkinson's disease-related C-terminal truncations, J. Mol. Biol 431 (2019) 3913–3919. [PubMed: 31295458]

[13]. Guerrero-Ferreira R, Taylor NM, Arteni AA, Kumari P, Mona D, Ringler P, Britschgi M, Lauer ME, Makky A, Verasdonck J, Riek R, Melki R, Meier BH, Bockmann A, Bousset L, Stahlberg H. Two new polymorphic structures of human full-length alpha-synuclein fibrils solved by cryo-electron microscopy, Elife 8 (2019) 10.7554/eLife.48907.

[14]. Guerrero-Ferreira R, Taylor NM, Mona D, Ringler P, Lauer ME, Riek R, Britschgi M, Stahlberg H. Cryo-EM structure of alpha-synuclein fibrils, Elife 7 (2018) 10.7554/eLife.36402.

[15]. Strohäker T, Jung BC, Liou SH, Fernandez CO, Riedel D, Becker S, Halliday GM, Bennati M, Kim WS, Lee SJ, Zweckstetter M. Structural heterogeneity of α-synuclein fibrils amplified from patient brain extracts, Nat. Commun 10 (2019) 5535–w. [PubMed: 31797870]

[16]. Schweighauser M, Shi Y, Tarutani A, Kametani F, Murzin AG, Ghetti B, Matsubara T, Tomita T, Ando T, Hasegawa K, Murayama S, Yoshida M, Hasegawa M, Scheres SHW, Goedert M.

Structures of alpha-synuclein filaments from multiple system atrophy, Nature 585 (2020) 464–469. [PubMed: 32461689]

[17]. Giasson BI, Forman MS, Higuchi M, Golbe LI, Graves CL, Kotzbauer PT, Trojanowski JQ, Lee VM. Initiation and synergistic fibrillization of tau and alpha-synuclein, Science 300 (2003) 636–640. [PubMed: 12714745]

[18]. Kam TI, Mao X, Park H, Chou SC, Karuppagounder SS, Umanah GE, Yun SP, Brahmachari S, Panicker N, Chen R, Andrabi SA, Qi C, Poirier GG, Pletnikova O, Troncoso JC, Bekris LM, Leverenz JB, Pantelyat A, Ko HS, Rosenthal LS, Dawson TM, Dawson VL. Poly(ADP-ribose) drives pathologic α-synuclein neurodegeneration in parkinson's disease, Science 362 (2018) eaat8407. doi: 10.1126/science.aat8407. [PubMed: 30385548]

[19]. Galvagnion C, Buell AK, Meisl G, Michaels TC, Vendruscolo M, Knowles TP, Dobson CM. Lipid vesicles trigger α-synuclein aggregation by stimulating primary nucleation, Nat. Chem. Biol 11 (2015) 229–234. [PubMed: 25643172]

[20]. Sengupta U, Puangmalai N, Bhatt N, Garcia S, Zhao Y, Kayed R. Polymorphic α-synuclein strains modified by dopamine and docosahexaenoic acid interact differentially with tau protein, Mol. Neurobiol 57 (2020) 2741–2765. [PubMed: 32350746]

[21]. Dasari AKR, Kayed R, Wi S, Lim KH. Tau interacts with the C-terminal region of α-synuclein, promoting formation of toxic aggregates with distinct molecular conformations, Biochemistry 58 (2019) 2814–2821. [PubMed: 31132261]

[22]. Ghee M, Melki R, Michot N, Mallet J. PA700, the regulatory complex of the 26S proteasome, interferes with alpha-synuclein assembly, Febs J. 272 (2005) 4023–4033. [PubMed: 16098186]

[23]. Despres C, Byrne C, Qi H, Cantrelle FX, Huvent I, Chambraud B, Baulieu EE, Jacquot Y, Landrieu I, Lippens G, Smet-Nocca C. Identification of the tau phosphorylation pattern that drives its aggregation, Proc. Natl. Acad. Sci. U. S. A 114 (2017) 9080–9085. [PubMed: 28784767]

[24]. Takegoshi K, Nakamura S, Terao T. ^{13}C–1H dipolar-driven ^{13}C–^{13}C recoupling without ^{13}C rf irradiation in nuclear magnetic resonance of rotating solids, The Journal of Chemical Physics 118 (2003) 2325–2341.

[25]. Gath J, Bousset L, Habenstein B, Melki R, Bockmann A, Meier BH. Unlike twins: An NMR comparison of two alpha-synuclein polymorphs featuring different toxicity, PLoS One 9 (2014) e90659. [PubMed: 24599158]

[26]. Bernado P, Bertoncini CW, Griesinger C, Zweckstetter M, Blackledge M. Defining long-range order and local disorder in native alpha-synuclein using residual dipolar couplings, J. Am. Chem. Soc 127 (2005) 17968–17969. [PubMed: 16366524]

[27]. Dedmon MM, Lindorff-Larsen K, Christodoulou J, Vendruscolo M, Dobson CM. Mapping long-range interactions in alpha-synuclein using spin-label NMR and ensemble molecular dynamics simulations, J. Am. Chem. Soc 127 (2005) 476–477. [PubMed: 15643843]

[28]. Fernandez CO, Hoyer W, Zweckstetter M, Jares-Erijman EA, Subramaniam V, Griesinger C, Jovin TM. NMR of alpha-synuclein-polyamine complexes elucidates the mechanism and kinetics of induced aggregation, Embo J. 23 (2004) 2039–2046. [PubMed: 15103328]

[29]. Lemkau LR, Comellas G, Lee SW, Rikardsen LK, Woods WS, George JM, Rienstra CM. Site-specific perturbations of alpha-synuclein fibril structure by the parkinson's disease associated mutations A53T and E46K, PLoS One 8 (2013) e49750. [PubMed: 23505409]

[30]. Kim C, Lv G, Lee JS, Jung BC, Masuda-Suzukake M, Hong CS, Valera E, Lee HJ, Paik SR, Hasegawa M, Masliah E, Eliezer D, Lee SJ. Exposure to bacterial endotoxin generates a distinct strain of alpha-synuclein fibril, Sci. Rep 6 (2016) 30891. [PubMed: 27488222]

[31]. Forman MS, Schmidt ML, Kasturi S, Perl DP, Lee VM, Trojanowski JQ. Tau and alpha-synuclein pathology in amygdala of parkinsonism-dementia complex patients of guam, Am. J. Pathol 160 (2002) 1725–1731. [PubMed: 12000724]

[32]. Castillo-Carranza DL, Guerrero-Munoz MJ, Sengupta U, Gerson JE, Kayed R. Alpha-synuclein oligomers induce a unique toxic tau strain, Biol. Psychiatry 84 (2018) 499–508. [PubMed: 29478699]

[33]. Gerson JE, Farmer KM, Henson N, Castillo-Carranza DL, Carretero Murillo M, Sengupta U, Barrett A, Kayed R. Tau oligomers mediate alpha-synuclein toxicity and can be targeted by immunotherapy, Mol. Neurodegener 13 (2018) 13–9. [PubMed: 29544548]

[34]. Clinton LK, Blurton-Jones M, Myczek K, Trojanowski JQ, LaFerla FM. Synergistic interactions between abeta, tau, and alpha-synuclein: Acceleration of neuropathology and cognitive decline, J. Neurosci 30 (2010) 7281–7289. [PubMed: 20505094]

[35]. Bhasne K, Sebastian S, Jain N, Mukhopadhyay S. Synergistic amyloid switch triggered by early heterotypic oligomerization of intrinsically disordered α-synuclein and tau, J. Mol. Biol 430 (2018) 2508–2520. [PubMed: 29704492]

[36]. Puentes LN, Lengyel-Zhand Z, Lee JY, Hsieh C, Schneider ME, Edwards KJ, Luk KC, Lee VM −, Trojanowski JQ, Mach RH. Poly (ADP-ribose) induces α-synuclein aggregation in neuronal-like cells and interacts with phosphorylated α-synuclein in post mortem PD samples, bioRxiv (2020) 2020.04.08.032250.

[37]. Iyer A, Roeters SJ, Kogan V, Woutersen S, Claessens M M A E, V. Subramaniam. C-terminal truncated alpha-synuclein fibrils contain strongly twisted beta-sheets, J. Am. Chem. Soc 139 (2017) 15392–15400. [PubMed: 28968082]

[38]. Gath J, Habenstein B, Bousset L, Melki R, Meier BH, Bockmann A. Solid-state NMR sequential assignments of alpha-synuclein, Biomol. NMR Assign 6 (2012) 51–55. [PubMed: 21744165]

[39]. Bousset L, Pieri L, Ruiz-Arlandis G, Gath J, Jensen PH, Habenstein B, Madiona K, Olieric V, Bockmann A, Meier BH, Melki R. Structural and functional characterization of two alpha-synuclein strains, Nat. Commun 4 (2013) 2575. [PubMed: 24108358]

[40]. Scheres SHW. Amyloid structure determination in RELION-3.1, Acta Crystallogr. D. Struct. Biol 76 (2020) 94–101. [PubMed: 32038040]

Highlights

- Tau monomers promote formation of α-synuclein filaments with a distinct morphology.
- Solid-state NMR structural analyses suggest that the tau-promoted α-synuclein filaments have distinct molecular conformations.
- Cryo-EM structure reveals that the N- and C-terminal regions of the tau-promoted α-synuclein filaments are different from those of the previously reported filaments.

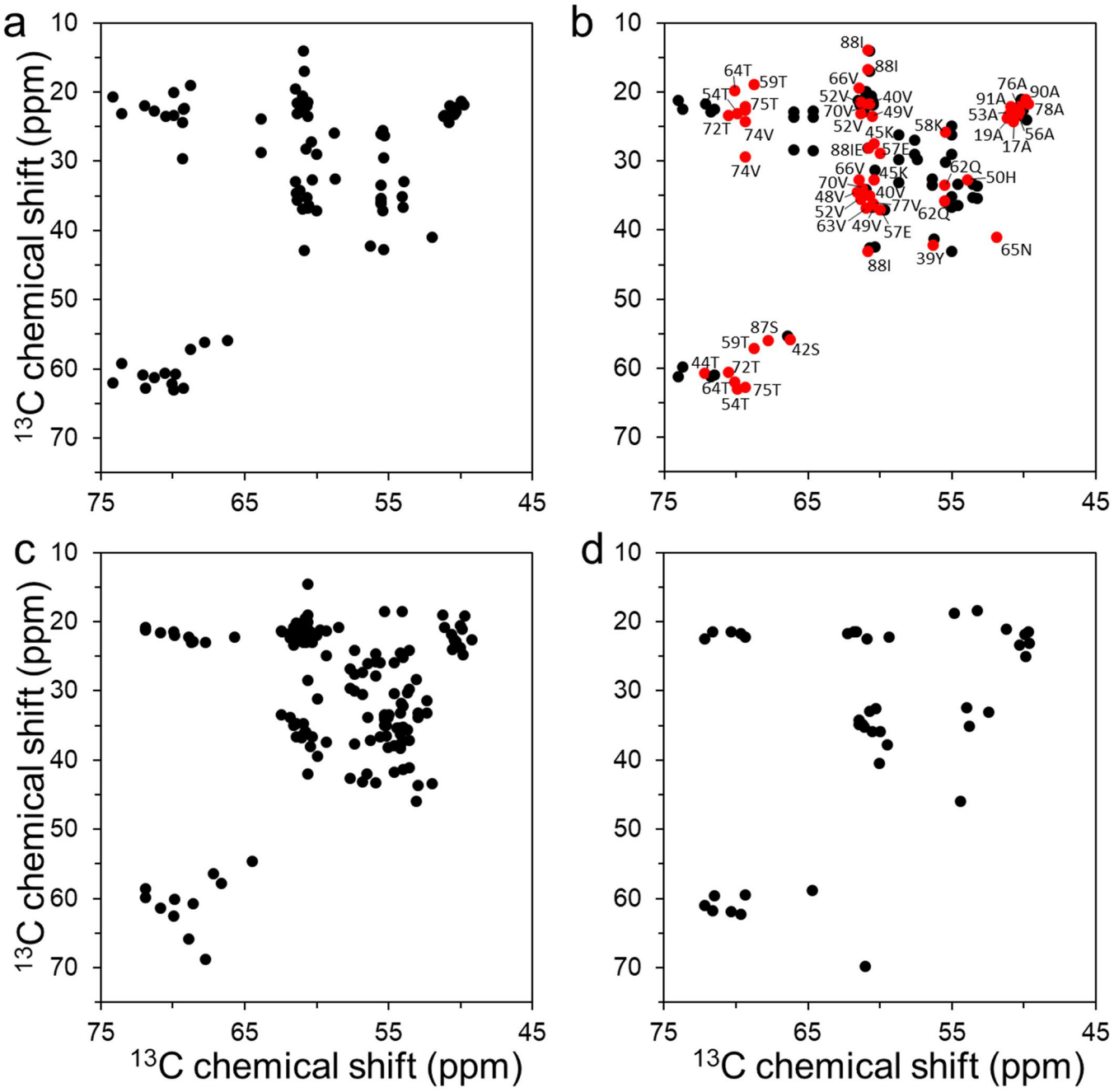

Figure 1.

Overview of aliphatic region of 2D ^{13}C - ^{13}C DARR NMR spectra of uniformly ^{13}C/^{15}N labeled α-synuclein filament polymorphs. (a) Tau-promoted α-synuclein polymorph. (b) Fibril-type α-synuclein polymorph (BMRB 18860).[25] Cross-peaks with similar NMR resonances for the tau-promoted α-synuclein polymorph and ribbon-type polymorph are colored in red with assignment (BMRB 18860). (c) Ribbon-type α-synuclein polymorph (BMRB 17498).[38] (d) Greek-key type α-synuclein polymorph (BMRB 25518).[9] The ribbon- and fibril-type polymorphs of α-synuclein have distinct molecular packing arrangement and intermolecular interactions.[25, 39] The NMR cross-peaks were drawn

using our experimental DARR spectrum for the tau-promoted filaments (a) and chemical shifts reported in BMRB for the previously reported DARR spectra of α-synuclein filaments (b – d).

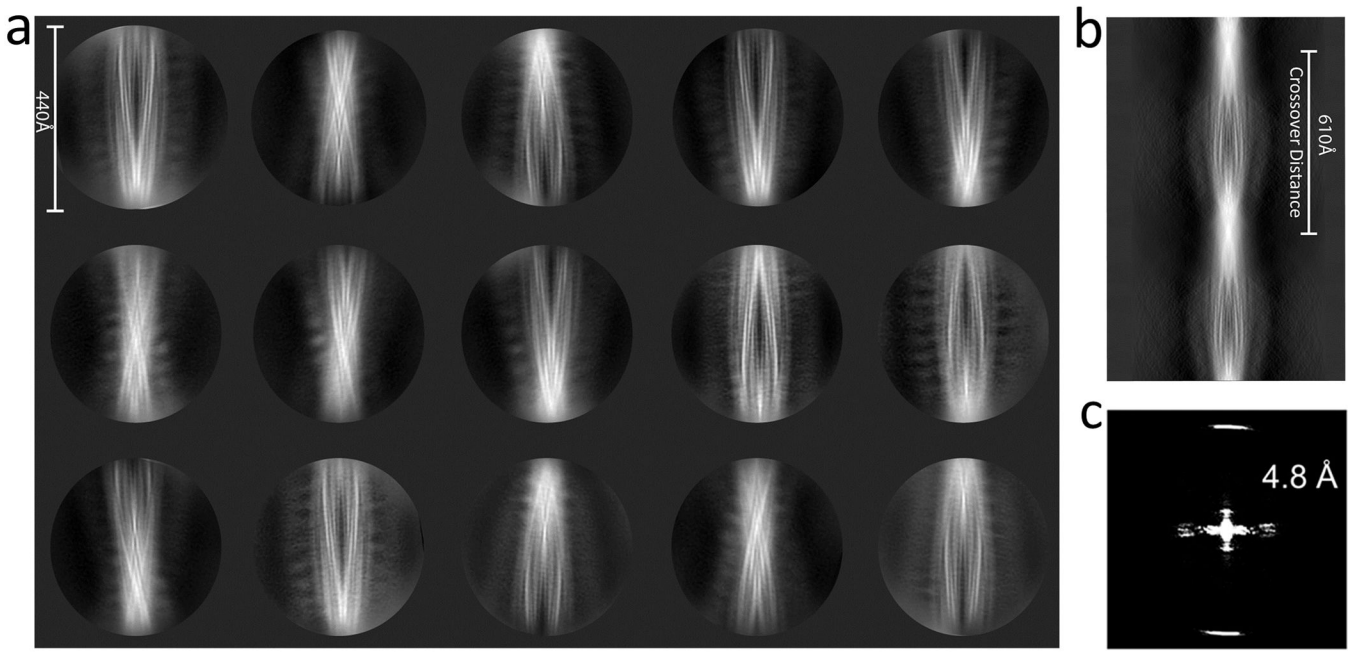

Figure 2.

2D class averages of the tau-promoted α-synuclein filaments. (a) Representative 2D class averages of the tau-promoted filaments using cisTEM (box size of 440 Å). (b) A sinogram representing the full rotation along the helical axis of the filament produced by relion_helix_inimodel2d as described by Scheres.[40] (c) The power spectrum of selected 2D reference-free class averages.

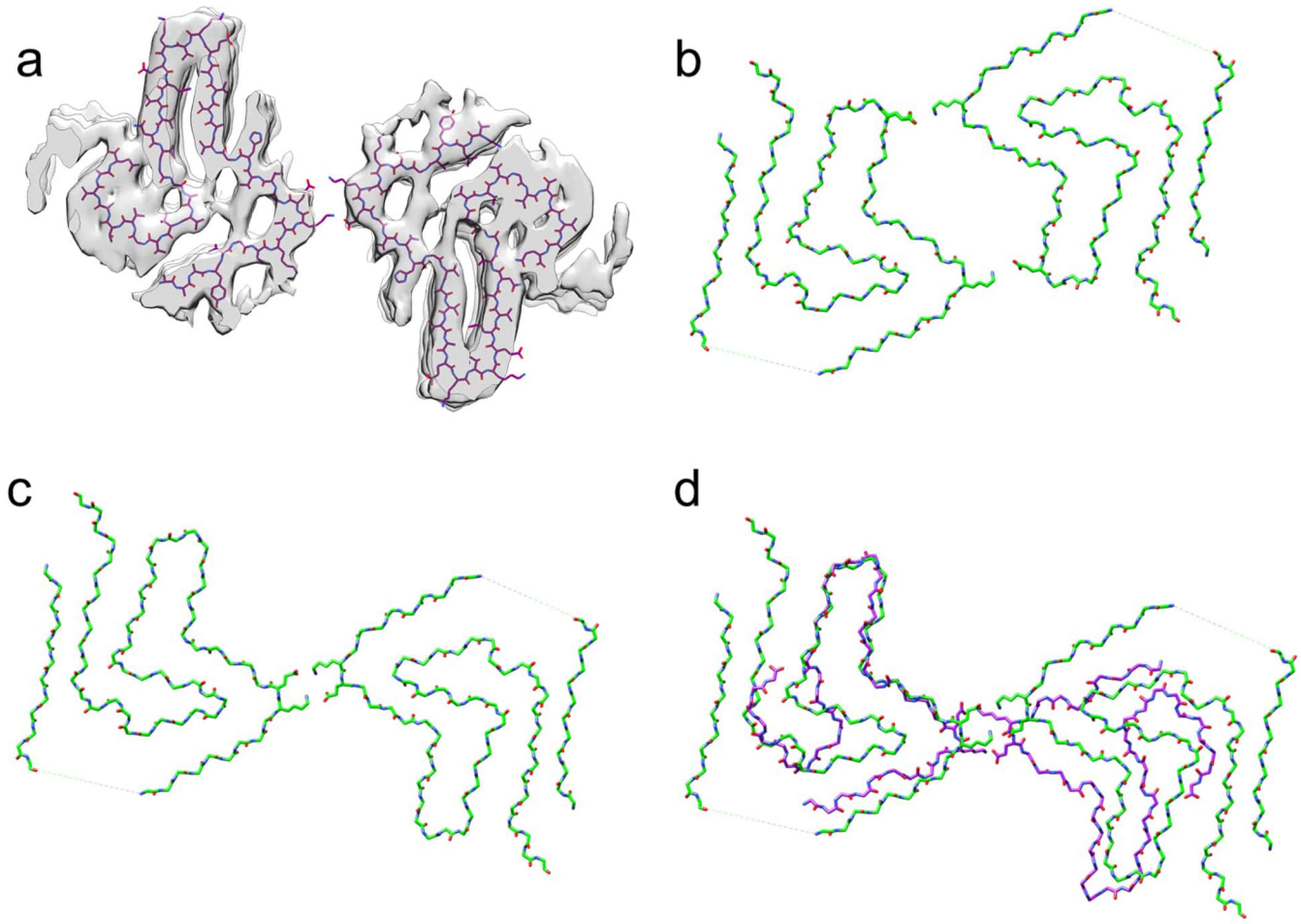

Figure 3.

Structural comparison of α-synuclein filament polymorphs. (a) Overlay of the tau-promoted α-synuclein filament atomic model on the density map. (b and c) α-synuclein filament polymorphs 2a and 2b, respectively, determined by previous cryo-EM structural studies.[13] (d) Overlaid structures of the tau-promoted α-synuclein filament (purple) and polymorph 2b (green). The same salt bridge between the residues K45 and E46 was observed in the interfacial region of the polymorph 2b (Figure 3c) and tau-promoted α-synuclein polymorph (Figure 3d).

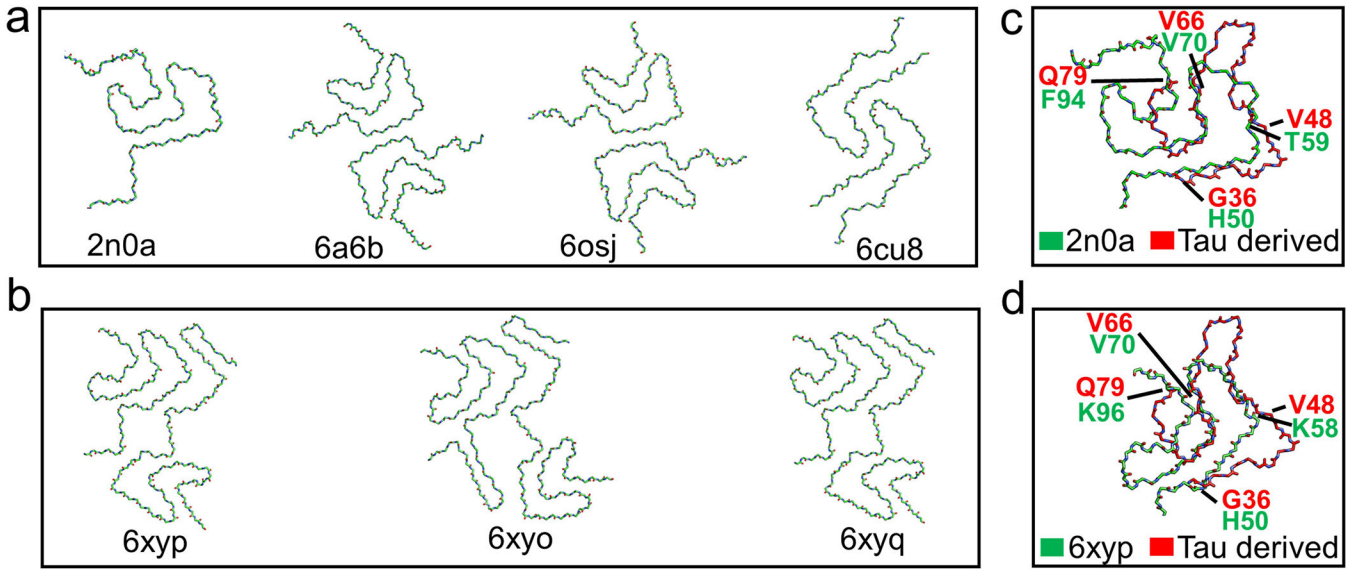

Figure 4.

Structural comparison of various polymorphs of full-length α-synuclein filaments. Representative structures of (a) α-synuclein polymorphs 1a (PDB 2n0a, 6a6b) [9, 10] and polymorph 1b (PDB 6cu8) [11]. (b) MSA patient derived α-synuclein polymorph type-1 (PDB 6xyp) and type-2 (PDB 6xyo, 6xyq).[16] (c and d) Overlay of the protofilament folds of the tau-promoted α-synuclein filament with polymorphs 1 and ex vivo MSA polymorphs, respectively.